Recruitment abundance index of Pacific bluefin tuna based on real-time troll monitoring survey data using Vector Autoregressive Spatio-Temporal (VAST) model analysis

Ko Fujioka, Saki Asai, Yohei Tsukahara,

Hiromu Fukuda and Shuya Nakatsuka

Highly Migratory Resources Division, Fisheries Resources Institute,

Japan Fisheries Research and Education Agency

2-12-4, Fukuura, Kanazawa-ku, Yokohama, Kanagawa 236-8648, JAPAN

Summary

In this study, we provided a recruitment abundance index of Pacific bluefin tuna using real-time troll monitoring (RTM) data instead of a traditional index based on sales slip data. The standardized CPUE based on RTM data for two periods of 2011-2023 and 2017-2023 fishing year was calculated by Vector Autoregressive Spatio-Temporal (VAST) model which is a delta-generalized linear mixed model that separately calculates the encounter probability and the positive catch rate. Estimated index for 2011-2023 showed a similar trend to the index based on traditional sales slip data for the overlap period (2011-2016). After the data-poor 2016 fishing year, in which operations were restricted due to a strict fishing regulation, our estimated RTM indices for each time period showed generally similar trend, thus the indices would be candidates for input into the stock assessment model. In addition, recent recruitment abundance indices suggested high value in the 2023 fishing year.

Introduction

The recruitment abundance index (i.e. standardized CPUE) based on troll fishery data is one of the most important input data for the Pacific bluefin tuna (PBF) stock assessment. The recruitment index has been developed using landing data in certain ports in Nagasaki prefecture in autumn-winter season, which is considered to represent the abundance of recruitment from two spawning grounds (Ichinokawa et al., 2012). However, Nishikawa et al. (2021) reviewed the fishery data for estimating abundance index and reported that calculated index might be negatively biased after 2016 due to the changes in fishery operation (increasing of the live release at sea) responding to management measures (e.g. minimum size limitation and substantial individual quota management) and thus it was not used for the stock assessment conducted in 2022. Therefore, PBFWG needs to explore/develop a recruitment abundance index using alternative data to sales slip data.

In the last stock assessment (ISC 2022), the recruitments from 2017 to 2020 were estimated based on mainly the assumed stock-recruitment relationship (SRR) since there were limited recruitment information in the base-case model, and consequently those were estimated as no deviations from the SRR. Additionally, real-time troll monitoring (RTM) survey data was also used in the sensitivity analysis of the assessment and projections as an alternative index to traditional troll index to seek the potential effect of the alternative index on the results of the current base case as well as the management advice based on that. Fukuda et al., (2021) reported that the estimated index using RTM data performs as well as traditional troll CPUE with ASPM-R model diagnostics. For the full stock

assessment in this 2024, it is desirable to input the reliable latest recruitment information into the model for the stock analysis to make the advice with consideration about the most recent recruitment figure.

Because of troll sales slip data was strongly affected by fishing regulations, the RTM survey index was submitted to the PBFWG as a candidate for alternative recruitment index (Fujioka et al., 2021, 2022, 2023). The RTM data provides geographic information on operations by vessels, allowing us to aggregate catch and effort data into a detailed latitude-longitude grids. Another advantage of the RTM data is that live release data and zero-catch operations can be obtained in a spatiotemporally fine-grained and timely manner (Tsukahara et al., 2019). However, as fishing regulations are tightened, even data from monitoring survey became sparse by fishing suspensions when fishing quotas (e.g. IQ; individual quota, local fisheries association based quota or area based quota, prefecture based quota) were exceeded throughout the fishing season. Therefore, in order to properly understand the recent trends of recruitment, Japan Fisheries Research and Education Agency (FRA) has started a scientific survey using charter operations of RTM vessels from the 2021 fishing year, adding to conventional RTM from 2011 by commercial vessels (Fig. 1). The chartered troll RTM operated in the same time and space (operating hours and area) as conventional RTM and are allowed to conduct IQ-independent research fishing. Fourteen RTM vessels were chartered to conduct survey operation for 10 days per four months from November to February with at least one operation in each month (Fujioka et al., 2022, 2023). A comparison of the spatio-temporal operational patterns of conventional RTM and charter RTM confirmed that their combined data interpolate each other's spatio-temporal strata (Fujioka et al., 2022, 2023).

In this working paper, we attempted to estimate recruitment indices for the entire period of troll RTM data collection from 2011 to 2023 and for the period of tightened fishing regulations from 2017 to 2023. Note that data for the February 2023 fishing year (February 2024) is currently being collected and is not included in the analysis. We explored area-weighted recruitment index using the spatio-temporal delta-generalized liner mixed modelling method (VAST: Vector Autoregressive Spatio-Temporal) (Thorson, 2019) with the expectation of reducing bias due to reduced sampling area caused by fishing regulations, according to the similar approach to Fujioka et al. (2021, 2022, 2023).

Methods

Data collection and summary

Data from 14 RTM vessels, which targeted for age-0 PBF (i.e. 40-60 cm fork length) during the

winter season (November to following February) in the East China Sea (ECS), have been collected since 2011 fishing year. The RTM data were collected in the same season and area as the traditional troll indices (sales slip basis) which represents the abundance of juvenile PBF born in both main spawning grounds in the North Western Pacific Ocean and the Sea of Japan. Locations of fishing port for those RTM vessels are shown in Figure 2. The number of RTM vessels increased to 14 vessels to date, and operational data were collected from 7 to 14 vessels each fishing year (Fig. 3). This paper updates the operational data by 14 vessels for the analysis period of 2011-2023 fishing year (Table 1). Since 2021 fishing year, in addition to conventional RTM, those conventional 14 RTM vessels were chartered for 10 days from November through February with at least one operation in each month to secure operations in the monitoring period, namely chartered RTM. They can operate independently with IQ as the catch from chartered operations were reported as part of the national government authorized FRA survey quota. Unless otherwise noted, the data from chartered RTM is included in the analysis.

RTM vessels are equipped with the GPS receiver and numeric keypad to input species and number of fish caught at the fishing location. The GPS data is recorded at intervals of 1 second during all trips. The vessel velocity can be estimated by the moving distance based on the GPS data. The estimated velocity was smoothed by the trimmed mean to exclude the obvious outlier due to the unsettled GPS data. These trace of fishing behavior and catch position can be used to estimate more precise efforts in an operation, i.e., actual operation time, than the catch per day used for sales slip data in the original index. PBF operation was defined as continuous vessel's velocity in the range of 2-7 knot for more than 30 minutes. The PBF catch and effort (residence time in minutes) data were aggregated in a 0.1×0.1 degree latitude/longitude grids and formatted into the following data; vessel name, year, month, day, latitude, longitude, catch, effort.

Data was carefully reviewed and any operations that were not clearly PBF operations based on the vessel's track and location records was removed by expert judgement. This is because fishermen may operate targeting other fish species due to changes in the catchability of PBF and/or demand for farming depending on year and season. We also excluded data that had obvious errors in the numeric keypad entry on board (e.g., more than 500 catches in one operation). Also, data in the northeastern part of Tsushima (latitude >34.5, longitude >129.2) was excluded (38 grids) because it was a unique

fishing ground only for the 2011 fishing year (Fujioka et al. 2021). This kind of data in rarely sampled area may affect the estimation of spatial effect of whole time series by the nature of VAST model for sharing information over space and time.

The spatial distribution of RTM operations by year is shown in Figure 4. Histograms of fishing effort (in minutes) and PBF catch records from 2011 to 2023 are shown in Figure 5. For the 0.1 degree grid aggregated data, the mean and standard deviation for fishing effort was 102.6 ± 105.2 minutes, ranging from 5 to 735 minutes. The mean and standard deviation of PBF catch was 3.6 ± 11.3 with a range of 0 to 284. For the entire period (2011-2023), the zero-catch rate operation was 66%, the positive catch rate was 34%, and the coefficient of variation of PBF catch (S.D./Mean) was 3.17. Nominal CPUE for each month and fishing year is shown in Figure 6. Table 2 also shows the latest 2023 data on monthly effort and grid for conventional and charter RTM operations.

Vector Autoregressive Spatio-Temporal (VAST) model

VAST is a delta-generalized linear mixed model that separately calculates the encounter probability and the positive catch rate, and is available from the R package "VAST" version 3.8.0 on the website (https://github.com/James-Thorson-NOAA/VAST) (Thorson, 2019). In our study, the encounter probability (p) at observation i was modeled using a logit-linked linear predictor, and the positive catch rate (r) at observation i was modeled using a log-linked linear predictor, as in the following equation:

(1) $\operatorname{logit}(p_i) = \beta_1(t_i) + L_{\omega 1}\omega_1(s_i) + L_{\varepsilon 1}\varepsilon_1(s_i, t_i) + \zeta_1(s_i, m_i) + L_{\eta 1}\eta_1(v_i)$

(2) $\log(r_i) = \beta_2(t_i) + L_{\omega 2}\omega_2(s_i) + L_{\varepsilon 2}\varepsilon_2(s_i, t_i) + \zeta_2(s_i, m_i) + L_{\eta 2}\eta_2(v_i)$

where $\beta(t_i)$ is the intercept in year t_i, $\omega(s_i)$ is the time-invariant spatial variations at location s_i, $\varepsilon(s_i, t_i)$ is the time-varying spatio-temporal variations at location s_i in year t_i, $\zeta(s_i, m_i)$ is the s_i month effect m_i as a catchability covariate which is either spatially varying at location at s_i or spatially constant by configuration and $\eta(v_i)$ is the effect of vessel v_i as a factor of overdispersion, and L_ω, L_ε and L_η are the scaling coefficients of the random effect distributions (Fujioka et al., 2021, 2022, 2023).

The probability of the density c is specified in this study as follows for a zero-inflated Poisson distribution:

$$(3)\ \Pr(c_i = c) = \begin{cases} 1 - p_i & \text{if } c = 0 \\ p_i \times ZeroInflated\ Poisson(c_i|\log(r_i), \sigma^2) & \text{if } c > 0 \end{cases}$$

where σ^2 is a dispersion parameter.

Then, the abundance index was predicted using an area-weighted approach, which calculates total abundance as a weighted sum of the estimated densities in a pre-defined spatial domain of knots. The number of knots was set equal to the number of observation locations (221 knots for 2011-2023).

Regarding the configuration of spatial structure with Gaussian Random Markov field (GRMR), this analysis used the anisotropic estimation of correlation, which estimate two different parameters for the correlation of two independent directions. In terms of temporal configuration, there is no assumption of correlated structure both year effect itself and spatio-temporal variation because the recruitment strength was highly variable over years based on the PBF assessment result.

Results and Discussion

This study provides updated data on RTM of age-0 PBF in the ECS (Fig. 2) during winter based on thirteen years (2011-2023) including the fishing regulation period. Operational data of RTM survey were obtained over 96-498 operational days with ranging 54-214 latitude/longitude grids from up to 14 vessels in each year (Table 1, Fig. 3). Since 2021 fishing year, IQ-independent charter RTM surveys were initiated to ensure sufficient operations in each spatial and temporal stratum. Fujioka et al. (2022, 2023) reported that two types of RTM data sets (chartered operation data and non-chartered operation data) for 2021 and 2022 were found to be useful that complement each other's spatio-temporal information. The operational patterns of conventional RTM and chartered RTM in the 2023 were also examined with a focus on the ratio of spatial grids to each other (Table 2). The results showed that the ratio of the number of spatial grids in the chartered survey to the number of spatial grids in the

conventional survey was sufficiently high (97.1% of the monthly total). In other words, the monthly spatial distribution of the chartered survey improves the data set for estimating recruitment abundance index.

Area-weighted standardized CPUEs for the entire period of 2011-2023 were estimated from spatio-temporal model analysis using the RTM vessel's data. The model excluded the vessel effect (Case 5) that assumed spatial and spatio-temporal effects, month effect as catchability covariate which was spatially varying for each of encounter probability and positive catch rate was judged to be the best model in terms of the AIC criteria (Table 3-1). The model converged successfully, with low final gradient values for each parameter (Table 4-1). Quantile diagnostics of these models also showed no considerable negative signs in the standardization (Fig. 11-1). The result of distance of 10% correlation of both encounter probability and positive catch rate was estimated as anisotropic shapes with approximately 25-65km of latitude axis mainly from south to north in each period of time (Fig. 8-1), so that the estimation in certain grids have some impacts on estimation in the approximately 2-6 grids away from there in 0.1 by 0.1 degree grid. This means that spatial correlation seems to be limited for availability of age-0 PBF. A longer period of data accumulation is needed to clarify the pattern of relationship between the PBF biomass distribution and the estimated biomass (Fig. 9-1, 10-1).

Similar to the period of 2011-2023, for the period of 2017-2023, the model (Case 5) was selected as the best model (Table 3-2). The model converged successfully, and the final gradients for each parameter were satisfactory for this 2017-2023 dataset, respectively (Table 4-2). Quantile diagnostics of these models also showed no considerable negative signs in the standardization each data period (Fig. 11-2). Decorrelation distance for different directions relative to encounter probability and positive catch rate are shown in Figure 8-2, and the patterns of center of the PBF biomass distribution in Figure 9-2, respectively. In this short period of time, Tsushima Islands in 2019-2020 and Goto Islands in 2022-2023 seemed to be the main distribution areas (Fig. 2), but further data accumulation is needed to determine a clear pattern with estimated biomass (Fig. 10-2) because the trend changes from year to year based on long-term data (Fig. 9-1, 10-1).

The comparison of the standardized indices by VAST (Case 5 for 2011-2023, Case 5 for 2017-2023) and traditional GLM index is shown in Figure 12. Trends for the two indices estimated in this study after 2016 were generally similar, with the long-term index (2011-2023) being slightly higher

7

than the short-term index (2017-2023). This difference in the scaled indices is considered due to the different scaling periods of data set between 2011-2023 and 2017-2023. It should also be emphasized that the estimated indices for 2011-2023 were quite similar to the traditional sales slip index throughout the overlapping period (2011-2016). If the PBFWG requests recruitment indicator before 2017 period in the stock assessment analysis, RTM indices would be available for the longer time series (2011-2023) as well as for the strict catch regulation period (2017-2023). The RTM indices since 2021 were robust whichever using chartered RTM data or not, and the index with the chartered RTM data showed smaller CV than that without the chartered RTM data (Fujioka et al., 2023). It suggested that adding to chartered RTM data to conventional RTM data are considered reasonable.

In conclusion, our estimated RTM index has a better use of available information than the traditional troll CPUE index of sales slip basis while showing a similar trend, and can be switched to an earlier year (i.e. 2011), which would inform the stock assessment model about the relative strength of recruitment at a higher resolution.

References

Fukuda, H., Fujioka, K., Tsukahara, Y., Nishikawa, K. and Nakatsuka, S. 2021. Reinforcement of Japanese PBF recruitment monitoring program. ISC/21/PBFWG-1/06.

Fujioka, K., Tsukahara, Y., Asai, S., Nishikawa, K., Fukuda, H. and Nakatsuka, S. 2021. Estimation of recruitment index of Pacific bluefin tuna based on real-time troll monitoring survey data using Vector Autoregressive Spatio-Temporal (VAST) model analysis. ISC/21/PBFWG-02/03.

Fujioka, K., Tsukahara, Y., Asai, S., Fukuda, H. and Nakatsuka, S. 2022. Update of estimated recruitment index of Pacific bluefin tuna based on real-time troll monitoring survey data, added IQ-independent scientific survey data for 2021. ISC/22/PBFWG-02/01.

Fujioka, K., Tsukahara, Y., Asai, S., Fukuda, H. and Nakatsuka, S. 2023. Recruitment abundance index of immature Pacific bluefin tuna, derived from real-time monitoring survey data of troll fisheries. ISC/23/PBFWG-01/03.

Ichinokawa, M., Oshima, K. and Takeuchi, Y. 2012. Abundance indices of young Pacific bluefin tuna, derived from catch-and-effort data of troll fisheries in various regions of Japan. ISC/12/PFWG-1/11.

ISC 2022. Report of the Pacific bluefin tuna working group intersessional workshop. ISC/22/ANNEX/06.

Nishikawa, K., Tsukahara, Y., Fujioka, K., Fukuda, H. and Nakatsuka, S. 2021. Update of age-0 PBF index based on catch per unit effort data from Japanese troll fishery and its associated issues. ISC/21/PFWG-1/05.

Thorson, JT. 2019. Guidance for decisions using the Vector Autoregressive Spatio-Temporal (VAST) package in stock, ecosystem, habitat and climate assessments. *Fish. Res.* 210: 143-161.

Tsukahara, Y. and Chiba, K. 2019. Real-time recruitment monitoring for Pacific bluefin tuna using CPUE for troll vessels: Update up to 2018 fishing year. ISC/19/PBFWG-1/04.

Table 1 (a) Total number of efforts (in days) and (b) number of latitude/longitude grids (in 0.1 grid units) by 7-14 real-time troll monitoring vessels per month from 2011 to 2023 fishing year.

a) Total number of troll operations (days)

	2011	2012	2013	2014	2015	2016	2017	2018	2019	2020	2021	2022	2023
November	31	67	27	42	113	64	57	67	35	30	90	49	23
December	99	93	67	71	163	53	39	112	88	49	165	76	92
January	58	58	110	120	107	80	0	132	176	30	114	99	92
February	74	0	90	20	115	74	0	120	107	23	121	81	
Total	262	218	294	253	498	271	96	431	406	132	490	305	207

b) Total number of troll operations (grids)

	2011	2012	2013	2014	2015	2016	2017	2018	2019	2020	2021	2022	2023
November	22	30	29	27	43	31	24	31	25	25	48	26	22
December	50	64	40	54	75	40	30	28	30	36	69	46	45
January	68	68	71	91	42	38	0	62	30	32	59	44	41
February	64	0	63	36	52	62	0	63	44	29	38	49	
Total	204	162	203	208	212	171	54	184	129	122	214	165	108

Table 2 Monthly effort (in days) and grid (in 0.1 grid units) of conventional real-time monitoring and chartered real-time monitoring by 14 troll vessels in the 2023 fishing year. Both monitoring surveys were conducted by the same 14 troll vessels. Note that data for the February 2023 fishing year (February 2024) is currently being collected and is not included in the analysis.

	Total operation		Conventional		Charter		Ratio of chater to conventional	
	days	grids	days	grids	days	grids	days (%)	grids (%)
November	23	22	8	10	15	12	187.5	120.0
December	92	45	50	27	42	31	84.0	114.8
January	92	41	52	31	40	23	76.9	74.2
February								
Total	207	108	110	68	97	66	88.2	97.1

Table 3-1 Combinations of explanatory variables for encounter probability (*p*) and positive catch (*r*) in a delta model and the values of Akaike information criterion (AIC) for the period 2011-2023. Delta AIC indicates the difference between the case 5 model with the lowest AIC. Blank means no convergence.

Case	Model for *p*	Model for *r*	AIC	*Δ* AIC
1	Yr + Station + Yr:Station + Month(spatially varying) + Vessel	Yr + Station + Yr:Station + Month(spatially varying) + Vessel		
2	Yr + Station + Yr:Station + Month(spatially varying) + Vessel	Yr + Station + Yr:Station + Month(spatially constant) + Vessel	68592	830
3	Yr + Station + Yr:Station + Month(spatially constant) + Vessel	Yr + Station + Yr:Station + Month(spatially varying) + Vessel		
4	Yr + Station + Yr:Station + Month(spatially constant) + Vessel	Yr + Station + Yr:Station + Month(spatially constant) + Vessel	68641	879
5	**Yr + Station + Yr:Station + Month(spatially varying)**	**Yr + Station + Yr:Station + Month(spatially varying)**	**67762**	**0**
6	Yr + Station + Yr:Station + Month(spatially varying)	Yr + Station + Yr:Station + Month(spatially constant)	70095	2334
7	Yr + Station + Yr:Station + Month(spatially constant)	Yr + Station + Yr:Station + Month(spatially varying)		

Table 3-2 Continuing with the dataset for the period 2017-2023. Delta AIC indicates the difference between the case 5 model with the lowest AIC. Blank means no convergence.

Case	Model for *p*	Model for *r*	AIC	*Δ* AIC
1	Yr + Station + Yr:Station + Month(spatially varying) + Vessel	Yr + Station + Yr:Station + Month(spatially varying) + Vessel		
2	Yr + Station + Yr:Station + Month(spatially varying) + Vessel	Yr + Station + Yr:Station + Month(spatially constant) + Vessel	41682	680
3	Yr + Station + Yr:Station + Month(spatially constant) + Vessel	Yr + Station + Yr:Station + Month(spatially varying) + Vessel		
4	Yr + Station + Yr:Station + Month(spatially constant) + Vessel	Yr + Station + Yr:Station + Month(spatially constant) + Vessel	41748	746
5	**Yr + Station + Yr:Station + Month(spatially varying)**	**Yr + Station + Yr:Station + Month(spatially varying)**	**41002**	**0**
6	Yr + Station + Yr:Station + Month(spatially varying)	Yr + Station + Yr:Station + Month(spatially constant)	42926	1924
7	Yr + Station + Yr:Station + Month(spatially constant)	Yr + Station + Yr:Station + Month(spatially varying)	41025	22

Table 4-1 Initial and final condition of each parameter related to explanatory variables in the 2011-2023 period. The list of parameters is as follows: beta; intercept for 1st or 2nd linear predictor (1st; encounter probability, 2nd; positive catch rate) each fishing year (2011-2023), L_omega; spatial factors for 1st or 2nd linear predictor, L_epsilon; spatio-temporal factors for 1st or 2nd linear predictor, logkappa; decorrelation rate for 1st or 2nd linear predictor, log_sigmaPhi; conditional variance between each month for intercepts of 1st linear predictor

Parameter	Starting value	Lower boundary	Maximum likelihood estimation	Upper boundary	Final gradient
ln_H_input	-0.18170	-5	-0.18170	5	-2.25E-09
ln_H_input	-0.00416	-5	-0.00416	5	5.90E-09
beta1_ft_2011	-0.49544	-Inf	-0.49536	Inf	-4.28E-10
beta1_ft_2012	-1.06835	-Inf	-1.06819	Inf	4.28E-10
beta1_ft_2013	-0.51001	-Inf	-0.50992	Inf	4.89E-11
beta1_ft_2014	-0.97241	-Inf	-0.97223	Inf	-4.73E-10
beta1_ft_2015	-0.61055	-Inf	-0.61041	Inf	-3.90E-10
beta1_ft_2016	0.49138	-Inf	0.49144	Inf	-1.82E-09
beta1_ft_2017	0.57989	-Inf	0.58003	Inf	1.20E-09
beta1_ft_2018	-0.27694	-Inf	-0.27681	Inf	-4.40E-10
beta1_ft_2019	-0.94079	-Inf	-0.94063	Inf	3.65E-10
beta1_ft_2020	-0.67282	-Inf	-0.67276	Inf	-3.97E-10
beta1_ft_2021	0.49207	-Inf	0.49220	Inf	-3.40E-10
beta1_ft_2022	0.61091	-Inf	0.61100	Inf	-3.47E-10
beta1_ft_2023	1.41120	-Inf	1.41127		-4.67E-10
L_omega1_z	-1.05773	-Inf	-1.05774	Inf	8.32E-08
L_epsilon1_z	-0.78547	-Inf	-0.78547	Inf	1.32E-07
logkappa1	-2.92718	-4.790245	-2.92718	-1.17374	1.16E-07
log_sigmaPhi1_k	-0.67689	-Inf	-0.67689	Inf	-1.54E-09
log_sigmaPhi1_k	-0.47246	-Inf	-0.47248	Inf	-4.90E-10
log_sigmaPhi1_k	-0.10009	-Inf	-0.10009	Inf	-1.46E-09
beta2_ft_2011	-3.34573	-Inf	-3.34574	Inf	1.29E-09
beta2_ft_2012	-3.48700	-Inf	-3.48701	Inf	-2.87E-10
beta2_ft_2013	-2.91748	-Inf	-2.91749	Inf	2.34E-10
beta2_ft_2014	-4.31447	-Inf	-4.31449	Inf	6.49E-09
beta2_ft_2015	-3.89818	-Inf	-3.89820	Inf	4.77E-10
beta2_ft_2016	-3.13604	-Inf	-3.13607	Inf	7.80E-09
beta2_ft_2017	-2.86399	-Inf	-2.86399	Inf	-4.65E-09
beta2_ft_2018	-2.84731	-Inf	-2.84733	Inf	4.90E-09
beta2_ft_2019	-3.41930	-Inf	-3.41933	Inf	3.01E-09
beta2_ft_2020	-3.45448	-Inf	-3.45448	Inf	-2.94E-09
beta2_ft_2021	-2.61595	-Inf	-2.61596	Inf	3.67E-09
beta2_ft_2022	-3.23365	-Inf	-3.23367	Inf	2.18E-09
beta2_ft_2023	-2.54793		-2.54793		-2.67E-09
L_omega2_z	0.35070	-Inf	0.35071	Inf	-1.89E-08
L_epsilon2_z	-0.82932	-Inf	-0.82932	Inf	1.16E-07
logkappa2	-2.00351	-4.790245	-2.00352	-1.17374	2.18E-08
log_sigmaPhi2_k	-0.42301	-Inf	-0.42301	Inf	-4.90E-09
log_sigmaPhi2_k	-0.37031	-Inf	-0.37030	Inf	-1.25E-09
log_sigmaPhi2_k	-0.39801	-Inf	-0.39800	Inf	-1.11E-09

Table 4-2 Continuing with the dataset for the period 2017-2023.

Parameter	Starting value	Lower boundary	Maximum likelihood estimation	Upper boundary	Final gradient
ln_H_input	-0.24750	-5	-0.24750	5	-4.51E-09
ln_H_input	0.01427	-5	0.01427	5	7.54E-09
beta1_ft_2017	0.28542	-Inf	0.28542	Inf	7.06E-10
beta1_ft_2018	-0.39106	-Inf	-0.39105	Inf	1.71E-09
beta1_ft_2019	-1.03174	-Inf	-1.03175	Inf	-6.76E-10
beta1_ft_2020	-0.73942	-Inf	-0.73948	Inf	-3.73E-09
beta1_ft_2021	0.52084	-Inf	0.52085	Inf	1.43E-09
beta1_ft_2022	0.63545	-Inf	0.63546	Inf	1.43E-09
beta1_ft_2023	1.11841	-Inf	1.11838	Inf	-1.98E-09
L_omega1_z	-1.09690	-Inf	-1.09689	Inf	5.39E-09
L_epsilon1_z	0.93641	-Inf	0.93641	Inf	-1.74E-08
logkappa1	-2.92458	-4.766133	-2.92456	-1.174945	7.01E-09
log_sigmaPhi1_k	-0.68458	-Inf	-0.68459	Inf	-1.02E-09
log_sigmaPhi1_k	-0.19230	-Inf	-0.19233	Inf	9.13E-10
log_sigmaPhi1_k	-0.07062	-Inf	-0.07065	Inf	3.61E-10
beta2_ft_2017	-2.91602	-Inf	-2.91607	Inf	1.73E-09
beta2_ft_2018	-2.40453	-Inf	-2.40454	Inf	1.38E-09
beta2_ft_2019	-3.49960	-Inf	-3.49958	Inf	-1.45E-09
beta2_ft_2020	-3.59674	-Inf	-3.59674	Inf	-5.91E-10
beta2_ft_2021	-2.68224	-Inf	-2.68224	Inf	-1.82E-09
beta2_ft_2022	-3.25415	-Inf	-3.25424	Inf	9.30E-09
beta2_ft_2023	-2.37676	-Inf	-2.37678	Inf	1.86E-09
L_omega2_z	0.42922	-Inf	0.42922	Inf	-1.85E-08
L_epsilon2_z	0.99640	-Inf	0.99641	Inf	-6.43E-08
logkappa2	-2.45977	-4.766133	-2.45979	-1.174945	2.72E-08
log_sigmaPhi2_k	-0.13887	-Inf	-0.13886	Inf	-4.20E-09
log_sigmaPhi2_k	0.09475	-Inf	0.09475	Inf	-2.39E-09
log_sigmaPhi2_k	-0.30896	-Inf	-0.30895	Inf	-8.29E-10
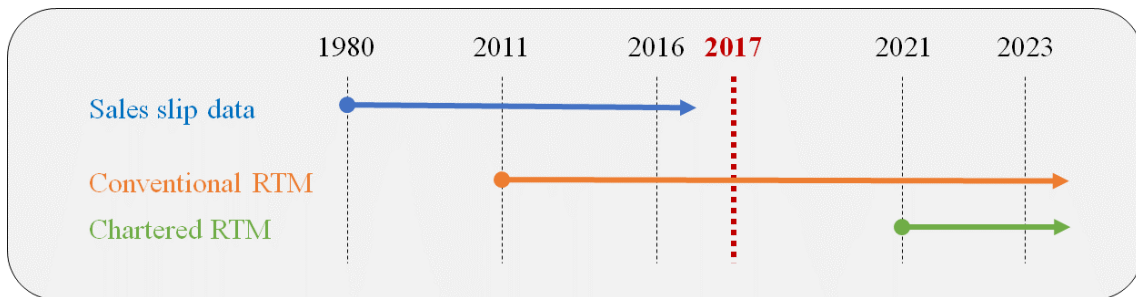
Figure 1 Three types of data collection of age-0 PBF from troll fisheries from 1980 to 2023 fishing year. The conventional real-time monitoring (RTM) and chartered RTM began in the 2011 and 2021 fishing year, respectively.
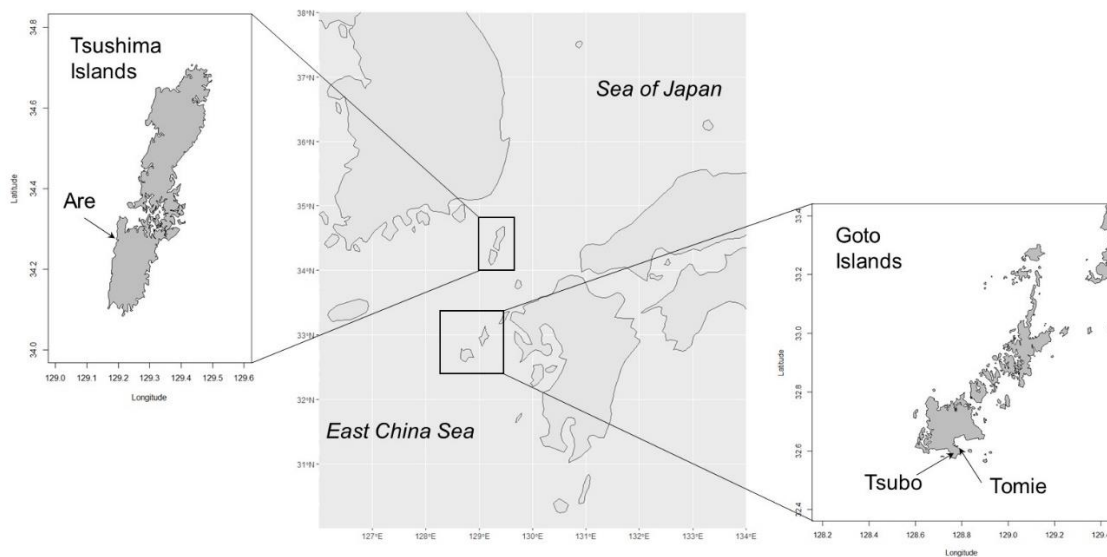
Figure 2 Location of fishing ports where real-time monitoring data of troll fisheries have been collected in Nagasaki prefecture. Left: 5 vessels in Izuhara-Are, Tsushima Islands. Right: 5 vessels in Goto-Tomie, and 4 vessels in Goto-Tsubo, Goto Islands.
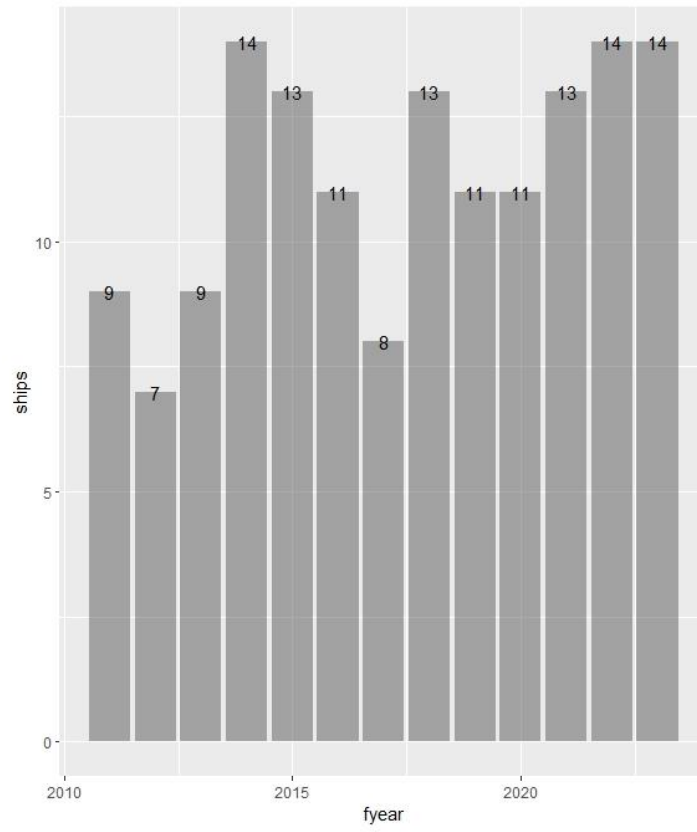
Figure 3 The number of real-time monitoring vessels with PBF operations from 2011 to 2023.
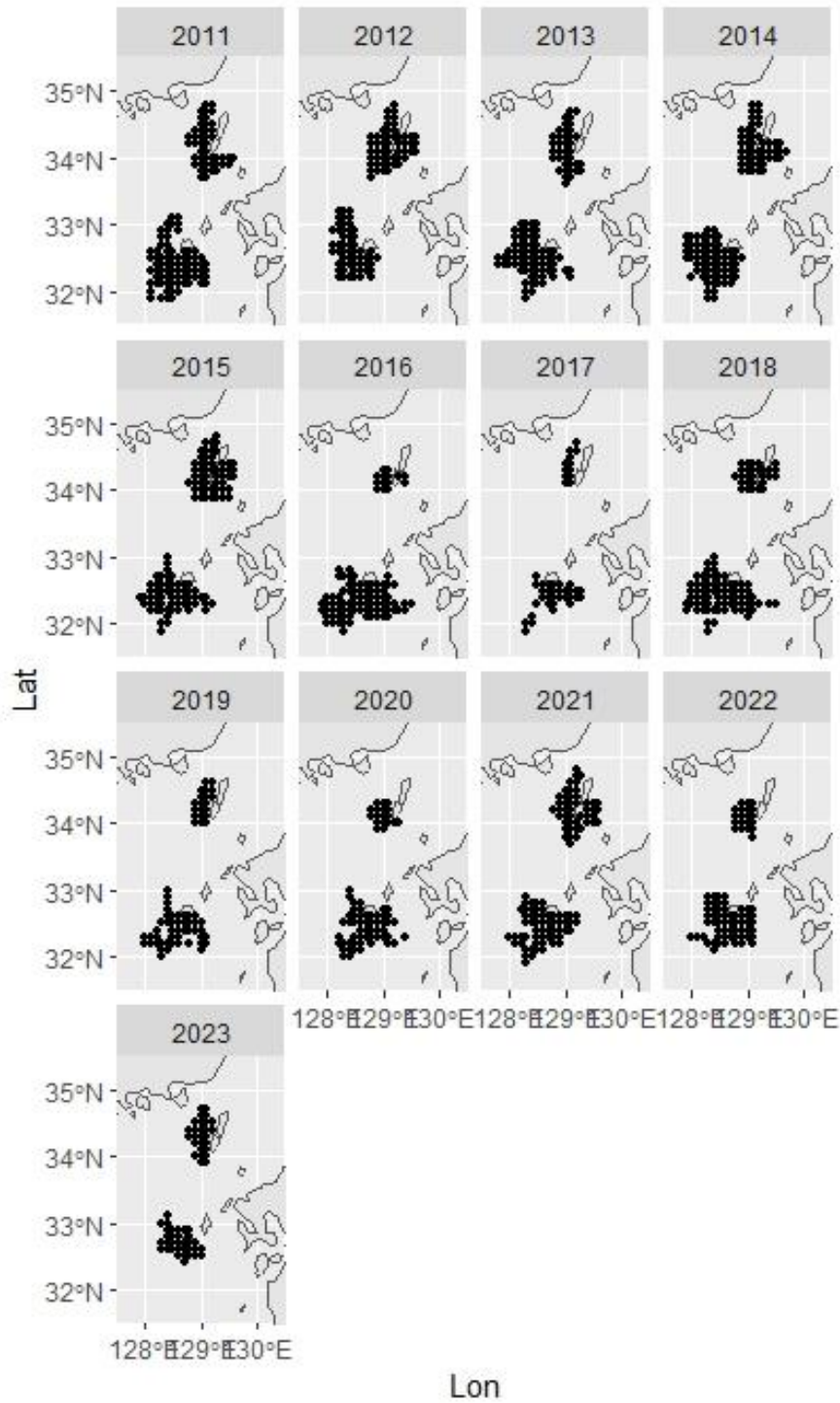
Figure 4 Distribution of troll operations of 7-14 real-time monitoring vessels from 2011 to 2023 fishing year for abundance estimation by the VAST model analysis. Data for the 2021-2023 fishing year includes chartered real-time monitoring in addition to conventional real-time monitoring.
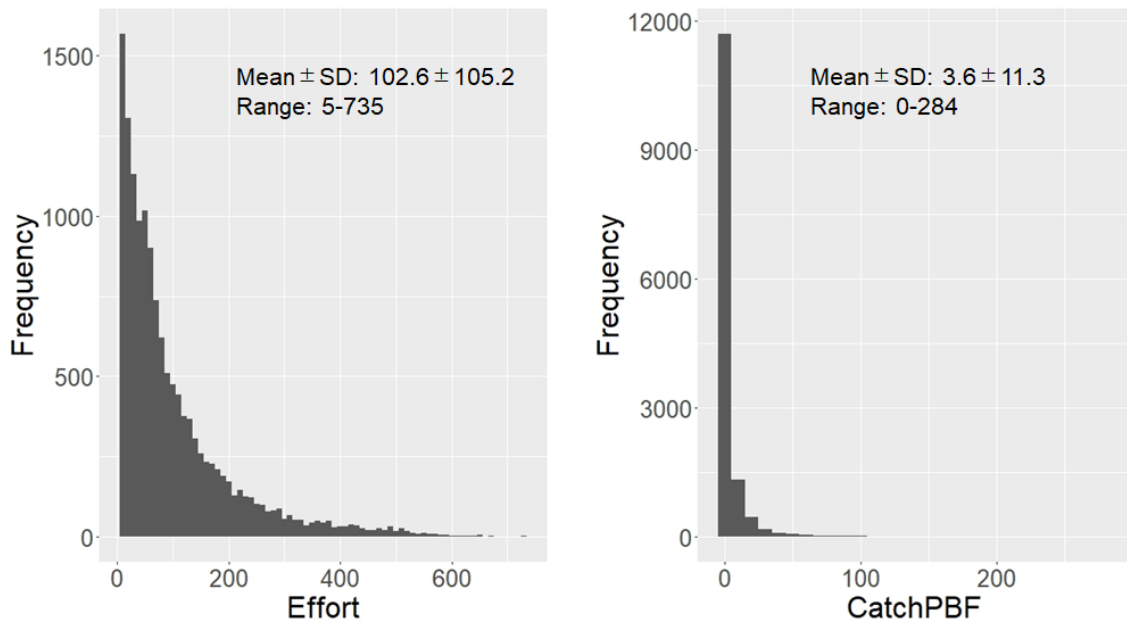
Figure 5 Frequency of fishing efforts (left) and PBF catches (right) for 2011-2023 based on 0.1 degree grid aggregate data.
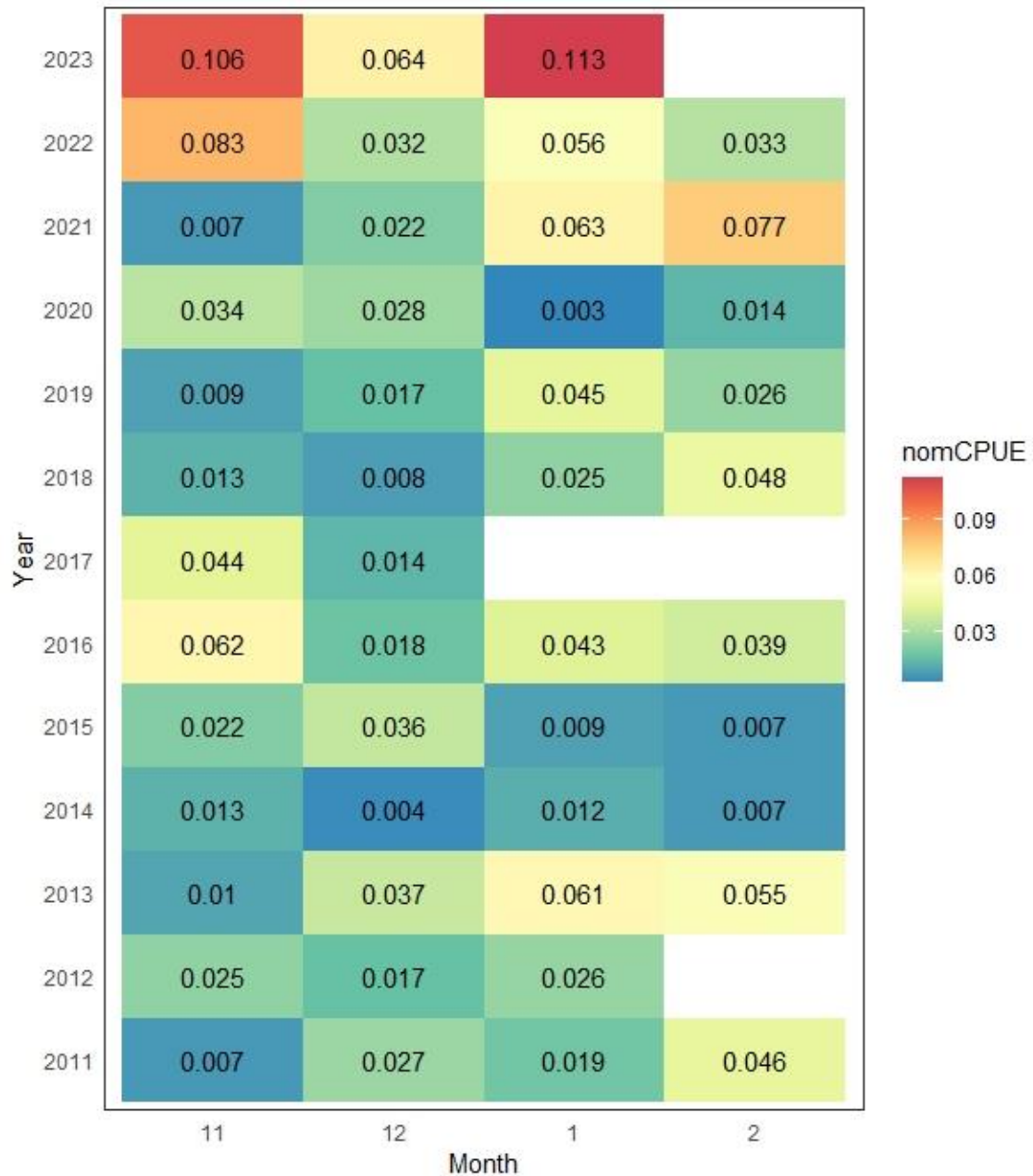
Figure 6 Nominal CPUE during 2011-2023 fishing year for each month (November to following February). No operations during the months of January and February of 2017 due to fishing regulations. Also, note that data for the February 2023 fishing year (February 2024) is currently being collected and is not included in the analysis.
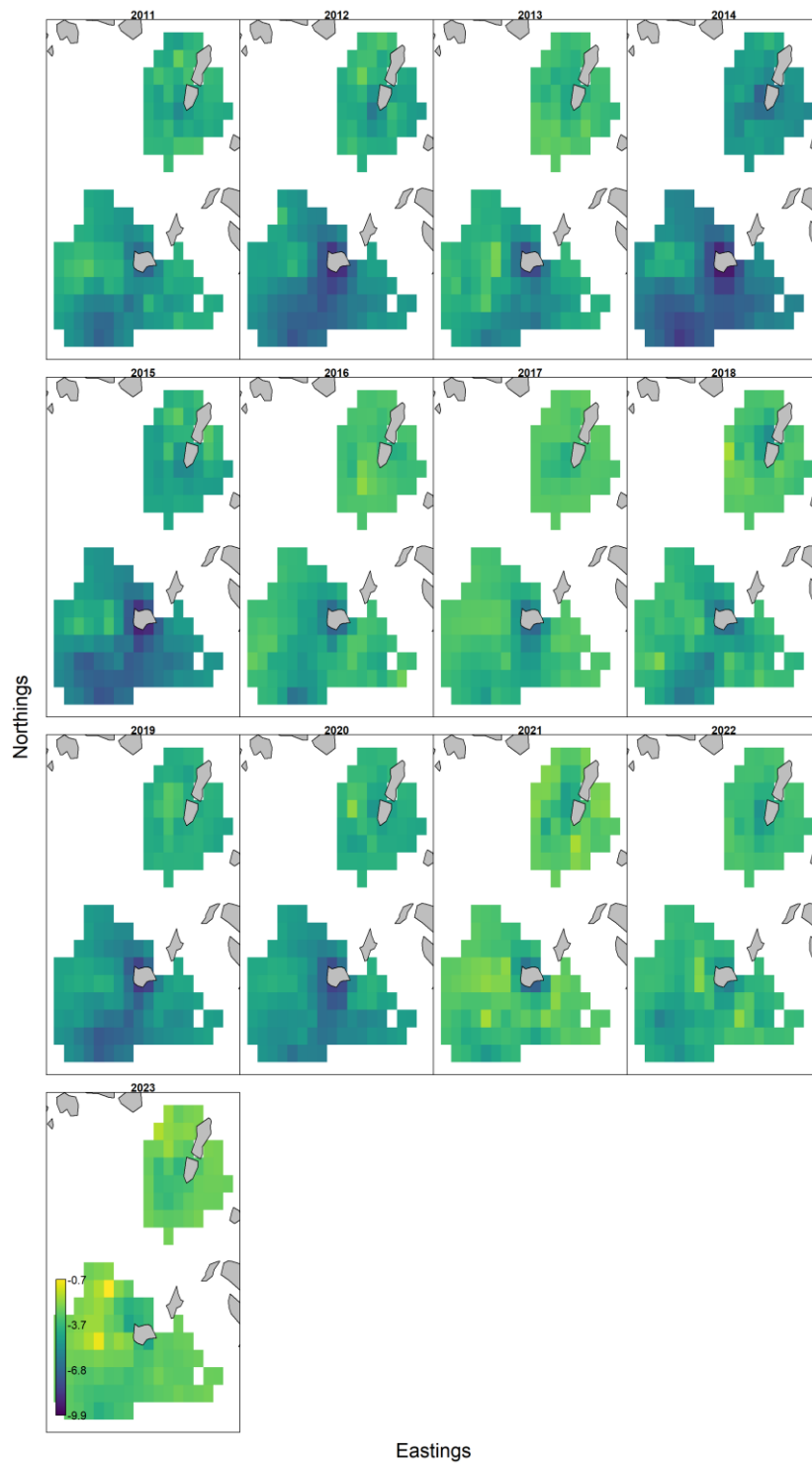
Figure 7-1 Spatio-temporal distribution of the log-transformed predicted densities of PBF for the 2011-2023 fishing year analyzed by VAST model. Warmer and cooler colors indicate high and low values, respectively.
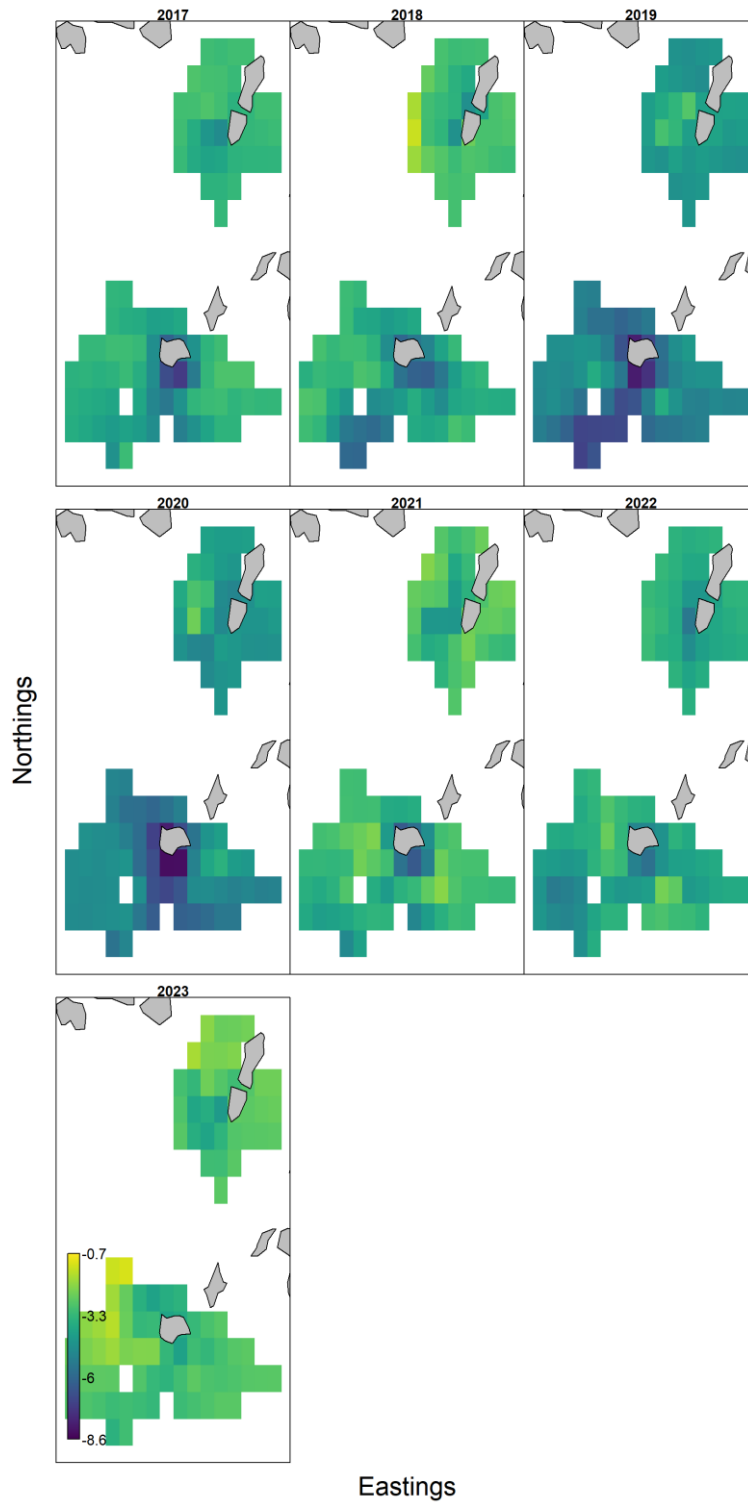
Figure 7-2 Continuing with the dataset for the period 2017-2023.

Distance at 10% correlation
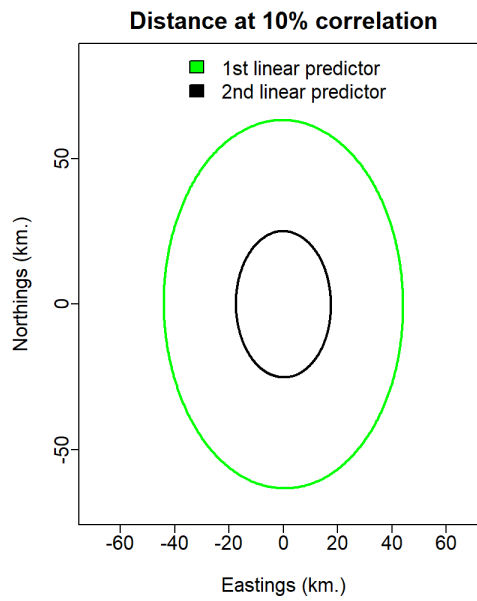
Figure 8-1 Decorrelation distance for different directions relative to encounter probability and positive catch rate for each of the two data periods 2011-2023. Indicating the magnitude of 2-dimensional spatial autocorrelation, and the ellipse signifies the distance (from a point located at position (0,0)), where the correlation drops to 10 %. The predicted densities correlated over a longer distance in the north-south direction than in the east-west direction.

Distance at 10% correlation
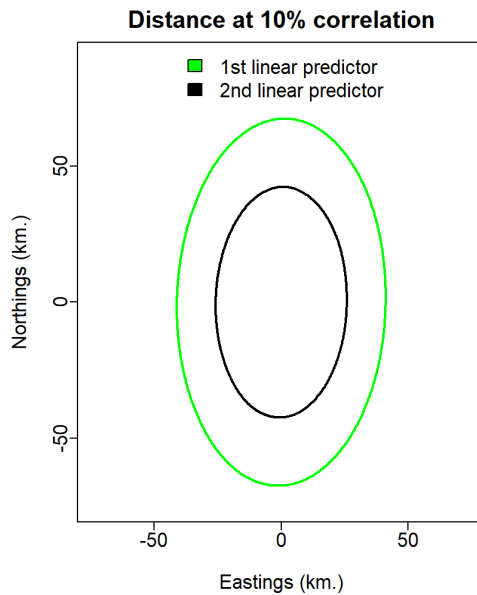
Figure 8-2 Continuing with the dataset for the period 2017-2023.

21
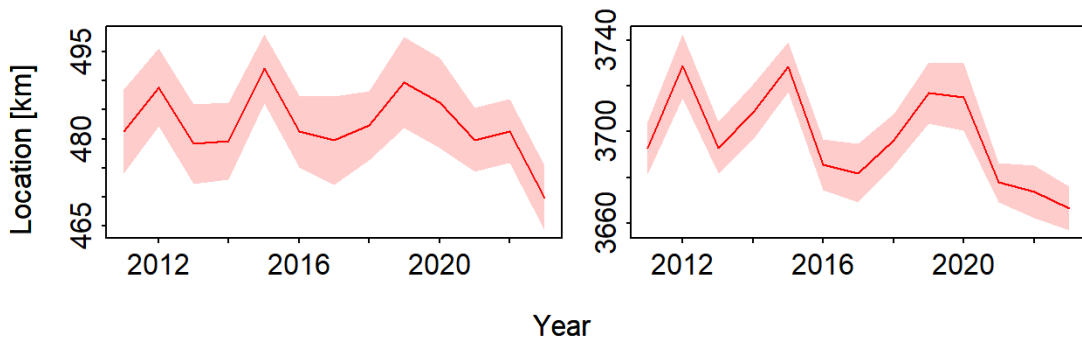
Figure 9-1 The center of gravity of PBF recruitments indicating the sift in distribution (distance (km)) in the east-west (left) and north-south (right) directions for the periods of 2017-2023. The thick line with shading indicates the mean value and standard error.
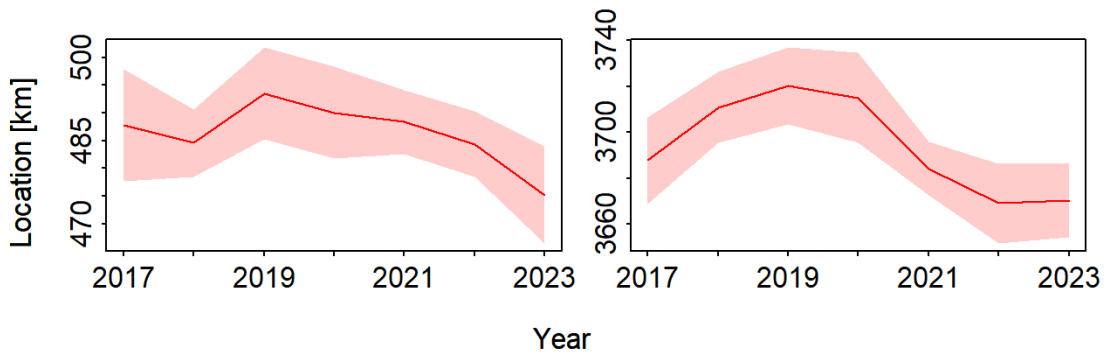
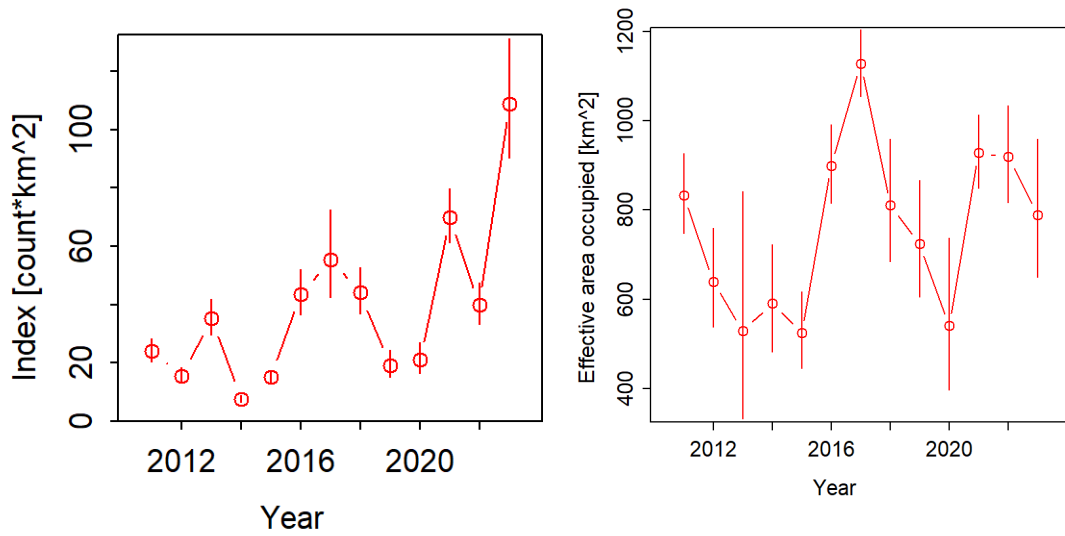**Figure 9-2** Continuing with the dataset for the period 2017-2023.

Figure 10-1 Standardized index of relative abundance of PBF (left) and estimated of the effective area occupied by PBF indicating range expansion/contraction (right) for the periods of 2011-2023. The open circles with vertical lines denote point estimates with standard errors.
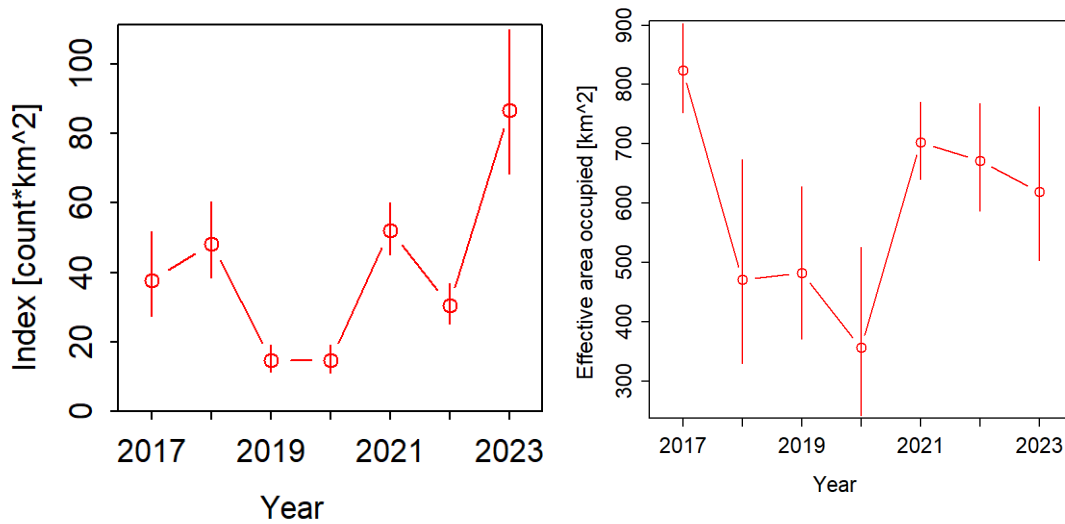
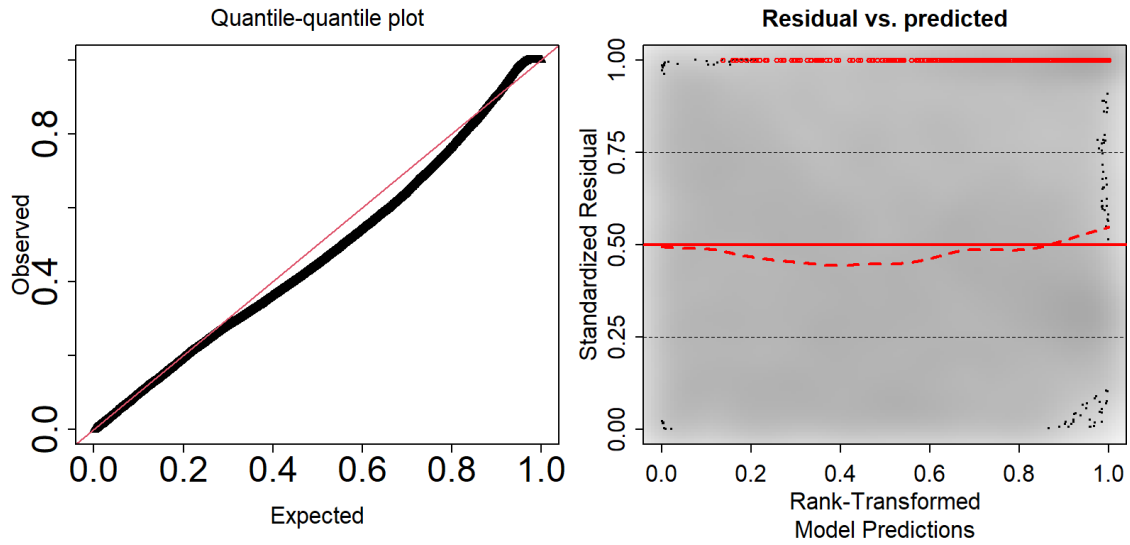**Figure 10-2** Continuing with the dataset for the period 2017-2023.

Figure 11-1 Diagnostic Q-Q plot (left) and residual plots (right) comparing the observed and predicted quantiles for the periods of 2011-2023. The residual plot calculating a quantile regression to compare the empirical 0.5 quantile in y-direction (dashed red lines) with the theoretical 0.5 quantile (red solid line).
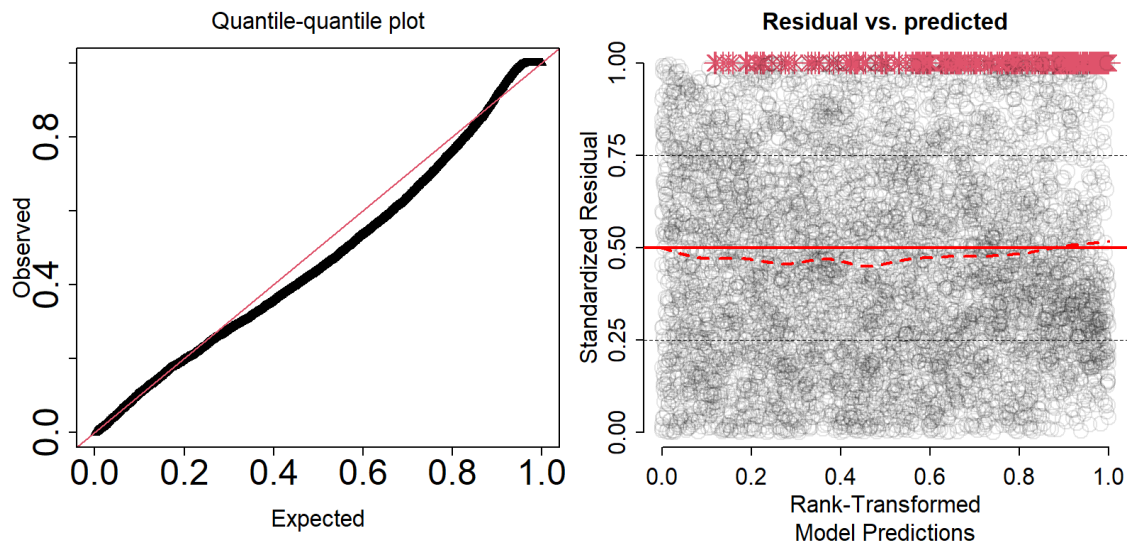

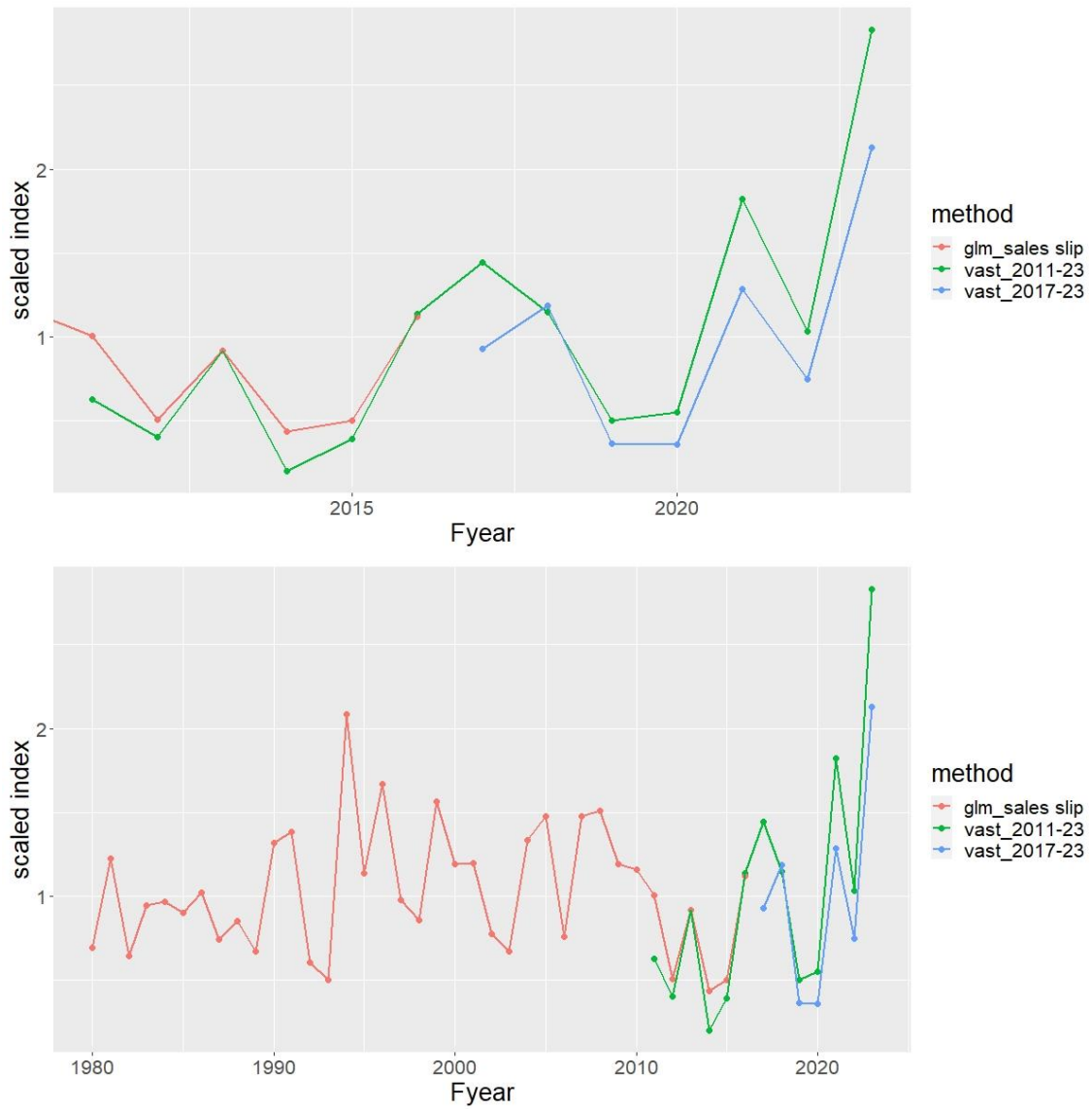**Figure 11-2** Continuing with the dataset for the period 2017-2023.

Figure 12 Recent trends of scaled abundance indices on results both traditional GLM (red line) using sales slip data (Nishikawa et al., 2021) and VAST analyses using real-time monitoring data for the periods 2011-2023 (green line) and 2017-2023 (blue line) (top). Full time-series indices are shown in bottom figure.